

THE NATURE AND ORIGIN OF THE NON-VOID LY α CLOUD POPULATION

CURTIS V. MANNING

Astronomy Department, University of California, Berkeley, CA 94720

Draft version November 18, 2018

ABSTRACT

I continue my study of the low-redshift Ly α cloud population. Previous work showed how galaxy catalogs could be used to attribute relative degrees of isolation to low-redshift Ly α clouds found in HST/GHRS spectra. This enabled the separation of clouds into two distinct populations corresponding to two distinct environments, variously characterized as void/unshocked and non-void/shocked. Void clouds have a steep equivalent width distribution (*i.e.*, many smaller absorbers) while non-void clouds have a flat distribution. I show that N-body/hydro simulations of Ly α clouds are inconsistent with observations of the clouds as a function of their environments. Simulations fail to predict the existence of significant numbers of detectable void clouds, and incorrectly predict the characteristics of non-void clouds. Implicated in this failure is the so-called fluctuating Gunn-Peterson Approximation, FGPA, which envisions that Ly α absorbers are formed in the large-scale structures of coalescing matter. A recent paper (Manning) has modeled the void cloud population as sub-galactic perturbations that have expanded in response to reionization. It is notable that success in this modeling was contingent upon using the more massive *isothermal* halo in place of the standard Navarro, Frenk & White, for it was found that gravitational restraint on evaporation of baryons is key to producing detectable void absorbers. In this paper I extend my modeling of Ly α clouds to non-void clouds using the same basic cloud model. In the case of voids, clouds are in a quiescent environment, while non-void clouds are thought of as void clouds that have accreted to the denser, turbulent intergalactic medium surrounding galaxies, and so are subjected to bow shock stripping. Model void clouds are analytically shock stripped, and a column density spectrum (CDS) is derived, based on the same halo velocity distribution function as that used to explain the void CDS. The non-void CDS produced by shocked sub-galactic clouds are found to be capable of producing an excellent fit to the observed non-void CDS without recourse to the FGPA mechanism.

Subject headings: intergalactic medium — quasars:absorption lines – dark matter

1. INTRODUCTION

N-body simulations now occupy a prominent position in the field of astrophysics. Their results promulgate a picture of structure formation with which it is hard to argue. The reason for this is that, through a variety of means, simulations have been designed to be consistent with high-redshift Ly α forest spectra, and they are integrated into the body of what can only be termed the standard model. However, because of the way cloud simulations are compounded, the results at high redshift can hardly be cited as proof of the accuracy of their simulations – only of their self-consistency.

Recent simulations of Ly α clouds by Davé & Tripp (2001) have extended predictions of models down to a redshift of zero. On the basis of their simulations, they predict a column density spectrum (CDS) with a steep cumulative spectral slope¹, $\mathcal{S}_{sim} = -1.15 \pm 0.04$. Simulations generally show that Ly α forest absorbers arise from the mildly overdense, highly photoionized gas that traces the dark matter potentials of large-scale structures surrounding galaxy concentrations (Bi, 1993; Miralda-Escude et al., 1996; Weinberg et al., 1997; Croft et al., 1998; Riediger et al., 1998; Davé & Tripp, 2001). In this paper, I will generally refer to this as the *intergalactic medium* (hereafter IGM). This will be contrasted with the voids, which are not dom-

inated by galaxies. The mechanism for the formation of Ly α clouds in these simulations is the fluctuating Gunn-Peterson approximation (hereafter FGPA), as explained in Bi (1993); Weinberg et al. (1997); Croft et al. (1998); Davé & Tripp (2001). It is based on the assumption that gas is substantially stripped or evaporated from all smaller halos, forming a roughly homogeneous filament surrounding the fully non-linear coalescing structures. These simulations have never predicted a significant low-redshift population of Ly α clouds in voids; diffuse gaseous structures in voids disperse with the Hubble flow, and today would be essentially undetectable (Riediger et al., 1998; Davé et al., 1999).

At low-redshift, galaxy redshift catalogs can be used to assess the relative proximity of Ly α clouds to galaxies and their larger structures. By so doing, it will be possible to check on the detailed predictions of the simulations. Therefore, the study of low- z absorbers as a function of environment may provide a crucial test for the N-body/hydro simulations.

In Manning (2002) (hereafter Paper I), low- z Ly α absorber data (Penton et al., 2000) was used, together with galaxy redshift catalogs, to assess the relative isolation of low-redshift Ly α clouds. It was shown how the summed scalar tidal field in space could be calculated, so that the relative isolation of clouds could be evaluated. I used a limiting tidal field \mathcal{T}_{lim} to divide the cloud catalog into low, and high-tidal field catalogs. As with Paper I, the tidal field is given in units of inverse Hubble time squared,

¹The CDS, as well as the equivalent width distribution function, is well-fit by a power-law distribution. Thus the “slope” is the index of the power-law.

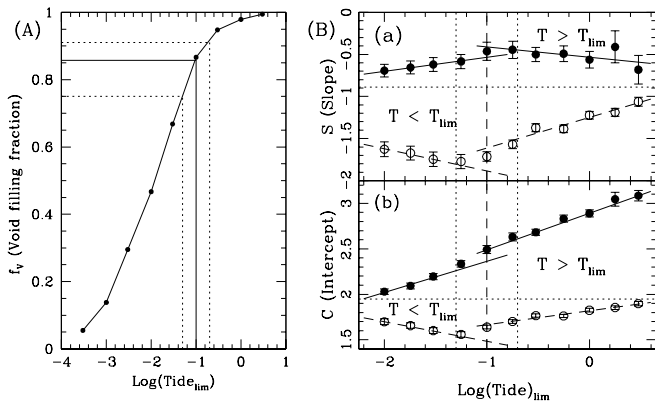


FIG. 1.— Panel A: The cumulative fraction of space in the survey (Penton et al., 2000) with tide $\mathcal{T} \leq \mathcal{T}_{lim}$. Assuming the sightlines are randomly selected, this is an estimate of the volume filling fraction with tide $\mathcal{T} \leq \mathcal{T}_{lim}$. The three vertical lines correspond to the “transition zone” shown in panel B, indicate the possible range in value of the void filling fraction. Panel B: The trend in slopes (panel a) and intercepts (panel b) of EWDFs defined by catalogs with tidal field $\mathcal{T} \leq \mathcal{T}_{lim}$ (top of each panel), or $\mathcal{T} > \mathcal{T}_{lim}$ (bottom), respectively, for the low- z cloud sample (see §6.2.1 Paper I). A strong transition in the slopes in the range $-1.3 \lesssim \log \mathcal{T}_{lim} \lesssim -0.7$ is apparent (two dotted vertical lines); also seen in the intercepts. See further discussion in Paper II.

resulting in a dimensionless parameter of order unity. The equivalent width distribution function (hereafter EWDF) of these catalogs appear to be well-fit by power-laws. I use the model, $\log d\mathcal{N}(\mathcal{W})/dz = \mathcal{C} + \mathcal{S} \log(\mathcal{W}/63 \text{ mÅ})$, where $\mathcal{N}(\mathcal{W})$ is the number of clouds per unit redshift with rest equivalent width $\geq \mathcal{W}$. Results of the fits can be seen in Fig. 1B (see caption). It was a surprise to find that a large population of clouds exist in extreme isolation. Void clouds have a steep EWDF ($\mathcal{S}_V \approx -1.6$), while non-void clouds have a flat slope ($\mathcal{S}_{NV} \approx -0.5$). Here and elsewhere I use the subscripts “V” and “NV” to stand for “void” and “non-void”. Thus there exist two separate populations of clouds. The trends of fitting parameters with variations in limiting tide \mathcal{T}_{lim} show that the two distinct types of clouds are separated by a transition zone (vertical dotted lines), whose width is plausibly caused by measurement errors, intrinsic scatter (in the Tully-Fisher relation), peculiar velocities of clouds and galaxies, and the spatial range a cloud travels during its transition from a void-type to a non-void-type galaxy. The dichotomy of types that is seen in this data, especially in the difference in slopes between void ($\mathcal{T} \leq \mathcal{T}_{lim}$), and non-void EWDFs ($\mathcal{T} \geq \mathcal{T}_{lim}$), is dramatic. There exists a similar dichotomy – unshocked *versus* shocked – found in the simulations of Riediger et al. (1998) and Cen & Ostriker (1999), suggesting that the phenomenology of non-void clouds may be explained in terms of shocks.

The cumulative distribution of tidal field strengths ($\mathcal{T} \leq \mathcal{T}_{lim}$) over the lines of sight from which the cloud data were taken (Penton et al., 2000) is shown in Fig. 1 panel A. It is used in conjunction with the range of values of \mathcal{T}_{lim} in the transition zone (Fig. 1 panel B) to assess the volume filling factor of voids. The center of the transition is taken to be the tidal field contour at which the shocked and unshocked populations meet. At $z \simeq 0$ the void filling

factor can be read off the figure;

$$f_V = 0.86^{+0.05}_{-0.11}, \quad (1)$$

in substantial agreement with the model of Cen & Ostriker (1999) ($\sim 90\%$). This is the fraction of the universe occupied by void-type clouds – hence the volume containing unshocked clouds. Void clouds have a steep slope that, according to the analysis of Manning (2003) (hereafter Paper II), requires clouds to have flat baryon distributions ($\rho_b \propto r^{-1.17}$), so that the observed absorption systems are detected at relatively large impact parameters (eg, $\langle r_p \rangle \sim 29$ kpc for $N_{HI} = 10^{13} \text{ cm}^{-2}$). In the shocked regions surrounding galaxy concentrations, such a diffuse structure would not be possible if significant cloud motions were present. Of course the logic behind expecting cloud motions is that the gravitational potentials of coalescing large-scale structure are driving them.

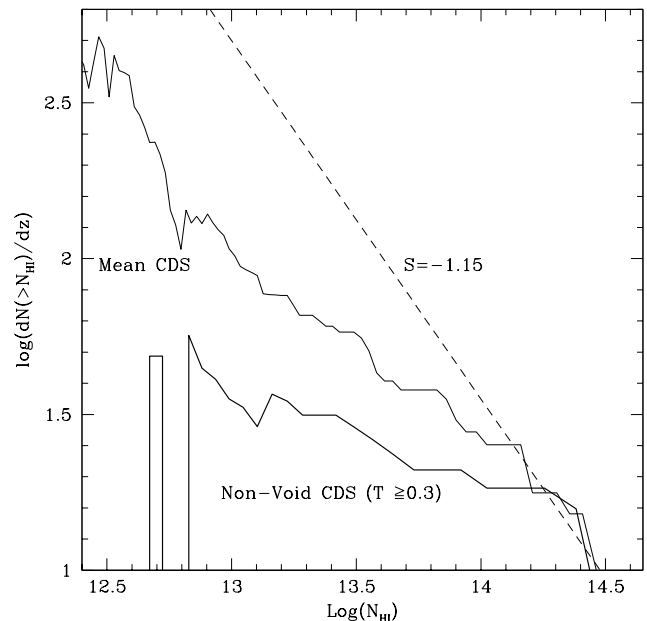


FIG. 2.— The column density spectrum of the non-void clouds (lower heavy line for $\mathcal{T} \geq 0.3$), shown in comparison to the mean CDS (light line). The dashed line represents the slope of the CDS predicted by Davé & Tripp (2001) for clouds that are expected to be found in regions of high tidal field. The non-void CDS has been adjusted to represent its line density to the CDS averaged over all space. Over *non-void* space, the non-void CDS has a ~ 7 times larger line density.

Because the N-body/hydro simulations have uniformly predicted that, at least at lower redshifts, Ly α absorbers occupy regions in proximity to galaxy concentrations, their predicted CDS spectral slope should agree with the observations of the local non-void clouds, since both are referring to clouds in the same locations². Fig. 2 is a comparison of predicted and observed spectral slopes. The dashed line represents the slope of the cumulative CDS prediction of Davé & Tripp (2001) with an arbitrary normalization. Also shown are CDS derived from EWDFs according to

²Simulations produce a CDS, while observations produce EWDFs. The blanketing that occurs in clouds that are not optically thin ($N_{HI} \gtrsim 10^{13.5}$; Fig 9 Paper II) results in spectral slopes of CDS being generally flatter than those of the corresponding EWDF.

the method of §5.3 of Paper II; the heavy line represents the CDS of non-void clouds ($\mathcal{T} \geq 0.3$), and the thin line is the *mean* CDS. The predicted slope of Davé & Tripp (2001), $\mathcal{S}_{sim} = -1.15 \pm 0.04$, does not compare well to the observed non-void EWDF slope, $\mathcal{S}_{NV} \simeq -0.5 \pm 0.1$ (Table 3 of Paper I), and agrees even less with the CDS slope $\simeq -0.36$. Analysis shows that *void* clouds are responsible for the steepness of the mean EWDF at $z \sim 0$; low EW clouds are quite rare in the turbulent IGM, as the cut-off in the non-void CDS in the Fig. 2 shows. But simulations have “detected” low-column density clouds in the IGM where observations suggest that their detection would be very difficult. This suggests that the analysis of Doppler parameters in standard N-body/hydro simulations is incorrect. I address this problem in more detail in §4.

The need to explain the void clouds, even while the standard model predicts no significant numbers, drives one to re-consider the predictions of the “fluctuating Gunn-Peterson approximation” (FGPA) (Bi, 1993; Weinberg et al., 1997; Croft et al., 1998; Davé & Tripp, 2001). But §2 of Paper II clearly showed that the predicted Doppler parameters for clouds in voids produced by this scenario exceed by far the observed *b*-values of void clouds from HST/GHRS spectra (Penton et al., 2000). Void clouds have Doppler parameters roughly half that of non-void clouds (Paper I). Clearly, this shows that void clouds cannot be expanding with the Hubble flow. If they are not produced by a fluctuating Gunn-Peterson effect, then how else does one explain void clouds except as discrete – *i.e.*, as subgalactic structures; remnant survivors from the reionization epoch?

In Paper II void Ly α clouds were modeled as gas associated with sub-galactic halos that has responded to the epoch of reionization by evaporating from their halos, albeit at a gravitationally restrained rate. A one-dimensional Lagrangian hydro code (Thoul & Weinberg, 1995) was used to track the evolution of the baryons following reionization at high resolution down to a redshift $z = 0$. The products of these simulations are used to calculate model CDS. Two different untruncated halo models are used, the Navarro et al. (1996, 1997) (NFW) halo, and an isothermal mass distribution ($\rho \propto r^{-2}$).

The NFW halo is the outcome of numerical simulations, and would seem to be the first choice for a model. However, in the analysis of Paper II, the NFW halo failed to restrain the evaporation of baryons sufficiently to produce measurable column densities in a void environment at $z = 0$. However, the isothermal halo proved viable as long as the distribution of cloud halo circular velocities were steep; consistent with that derived by Klypin et al. (1999); Klypin (2002) for isolated halos (see §6.2 of Paper II).

According to N-body simulations, an isolated galaxy should have a mass distribution in agreement with the NFW halo; a steep r^{-3} density profile for $r \gg r_{max}$. However, this conjecture is inconsistent with the findings that satellite galaxy distributions in groups and clusters follow an approximately inverse square number density relation with radius far beyond R_{max} or R_{vir} (Seldner & Peebles, 1977; McKay et al., 2002), and have velocity dispersions that are flat to similar distances (Zaritsky & White, 1994; Zaritsky et al., 1997; Zabludoff & Mulchaey, 2000; McKay et al.,

2002). These results are indicative of an isothermal, rather than an NFW mass distribution.

Recent re-thinking of the McKay et al. results (Prada & colleagues 2003) suggest the above results are affected by interloper galaxies which are randomly distributed in space (hence in velocity or redshift). However, that small galaxies are relatively unclustered, does not imply that they are randomly distributed: their conjecture is in strong contrast with findings that satellites have a number distribution $n \propto r^{-2.1}$ (McKay et al., 2002) around their primaries. Prada et al. claim also to have found a method to detect interlopers placed into simulated data that can then be applied to real data. It is odd that though interlopers are to be randomly inserted, their Fig. 3 shows a distinctly non-random distribution of interlopers. One wonders whether the algorithm for identifying interlopers has been applied in a way to pick out things inconsistent with the halo model. These doubts prompt the question of whether they merely “discovered” what they had presumed at the outset. This issue remains to be fully resolved, but for the present, I will consider the original work (McKay et al.) to be plausible, and probably correct in its essentials. In support of this are two points. First, this assumption is at least consistent with the results of Paper II that NFW halos were not good cloud models, and that isothermal halos are. Second, this particular assumption regarding the outer regions of galactic halos is not essential to the analysis, but it will be seen that it is consistent with other data to be developed in §4.3.

This same isothermal model is the basis of a successful explanation of the void EWDF. Perhaps non-void clouds may be explained by a similar approach.

The goal of the current paper is to explain the nature of non-void clouds. I do this in terms of the environment in which they are found. I here describe a theory in which non-void clouds are produced by discrete clouds. At the epoch of their formation, sub-galactic halos must have been distributed fairly evenly in the universe – approximately half in mildly overdense regions, and the other half in mildly underdense regions. As the universe evolved, the halos in overdense regions must be carried with the flow into the growing zones of shocked gas, as visual presentations of structure formation convincingly show. Thus, according to Birkhoff’s theorem (Birkhoff, 1923), underdense regions came to have a locally higher Hubble constant, which tends to promote the deepening of the underdensity, dispersing their halos and suppressing hierarchical growth. Of the halos that are now in non-void space, many may have arrived during the primary and secondary infall of the coalescing large-scale structure. At later times, when voids are well-established, the “gravitational-repulsion” (Piran, 1997) of the contents of voids requires that void clouds will be ejected at velocities dependent on void sizes and the values of the expansion parameter in the void.

Thus, the above reasoning strongly suggests that the great majority of current non-void clouds were, at one time or another, standard unshocked void clouds. Hence non-void clouds can be characterized with roughly the same halo velocity distribution function (HVDF) as derived for void clouds (Paper II), though the normalization will be different (see below).

The effect of the accretion of delicate void clouds to the shocked non-void space must be dramatic. When the

cloud encounters the dissipated gas in non-void space, the tenuously held gas is shock stripped, truncating the cloud, resulting in a modification of its EWDF. It is these effects that I intend to follow in this paper. The goal is to see if void clouds (*i.e.*, as sub-galactic structures), transformed by plausible shocks in the intergalactic medium, can be used to explain the non-void EWDF at low-redshift.

The cosmology assumed in this paper is that of Papers I and II – a standard flat lambda model with $h = 0.75$. The total matter density of voids is either referred to as $\Omega_V = \bar{\rho}_V/\rho_{crit}$, or as Ω_V/Ω_m , where $\Omega_m = 0.3$ is assumed. As in the other papers in this series, I assume the cosmic baryon density is $\Omega_b/\Omega_m = 0.1$. Recent results from the Wilkinson Microwave Anisotropy Probe (WMAP) (Spergel & colleagues, 2003) suggest a substantially larger value $\Omega_b/\Omega_m = 0.166$. The effects of the larger value will be noted. The large discovered line density and small Doppler parameters of void clouds (Papers I and II) strongly suggest that they are to a significant degree self-gravitating and discrete. I treat them as such herein.

I begin the analysis in §2 by studying the effects of shocks on model void clouds as a function of their velocity relative to the IGM. The non-void column density spectrum is modeled in §3. In §4 I discuss some of the broader issues touched upon in this paper, and summarize my findings in §5.

2. CONSTRAINING CLOUD VELOCITY

I model all Ly α absorbers as initially taking the form of void clouds, and therefore to be consistent with the models produced in Paper II. I view the difference in slopes between non-void EWDFs and void EWDFs as attributable to the relatively extreme conditions of the IGM – a denser, hotter, and turbulent environment. I propose that the primary factor in the modification of cloud characteristics is ram pressure from the relative motions of clouds through the IGM.

To constrain the rate of motion in the IGM to which clouds are subjected, I model the effects of shocks produced by clouds moving at a range of velocities within a medium of density ρ_{NV} . What ram pressure will explain the change in shape and relative normalization of the CDS? As noted above, this methodology assumes that the transition from void to non-void cloud characteristics is currently brought about by the impact of the clouds with the dissipated gas near the $\mathcal{T} = 0.1$ contour.

2.1. Shock Stripping of Void Clouds

Murakami & Ikeuchi (1994) (hereafter MI94) probed the effects of the stripping action of blast waves on mini-halos. Mini-halos (*e.g.*, Rees, 1986) were once utilized to explain the Ly α forest (Rees, 1986; Murakami & Ikeuchi, 1993), and are closely related to those sub-galactic halos studied in the present work. MI94 envisioned two phases of stripping – the first being the immediate result of the onset of the shock, and the second being the gradual stripping of the remnant by the relative velocity through the medium. MI94 found that the isothermal mini-halos suffer significant erosion during the initial shock only where the internal pressure of the cloud is less than the ram pressure. For the case of a cloud with velocity v_{cl} , encountering a dissipated medium with gas of density ρ_g the ram pressure

on the cloud is,

$$p_{ram} \equiv \rho_g v_{cl}^2. \quad (2)$$

MI94 showed that mini-halos could withstand the secondary stripping for a sustained amount of time if the escape velocity from the cloud were in excess of the oblique flow within the shock. Some clouds were seen to survive in excess of 3 Gyr.

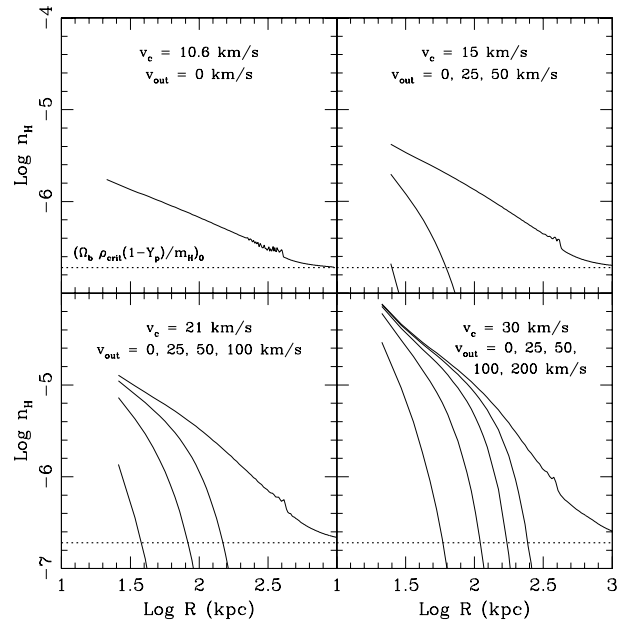


FIG. 3.— The density profiles of grown halos processed according to the prescription of Eq. 3 for various velocities v_{cl} (as noted in the panels). The dotted line represents the hydrogen density in the background (critical density) medium. When the cloud halo circular velocity $v_c = 10.6 \text{ km s}^{-1}$, the cloud is totally stripped even at $v_{cl} = 25 \text{ km s}^{-1}$. Larger clouds (higher v_c) survive larger ram pressures. In the final panel, cross-section of the $v_c = 30 \text{ km s}^{-1}$ cloud when $v_{cl} = 200 \text{ km s}^{-1}$ is only about 1/4 of that when $v_{cl} = 100 \text{ km s}^{-1}$.

The initial cloud models are produced according to the methods explained in §6 of Paper II. In these simulations, 200 baryonic bins are used. The first strip, which removes gas at pressures less than the ram pressure, can be implemented by the following transformation of density in each Lagrangian bin,

$$\rho(i) \implies \rho(i) e^{-(p_{ram}/p(i))}, \quad (3)$$

where the pressure in the cloud in the i th bin is $p(i)$. This formulation produces a fairly abrupt truncation of the baryon density where the cloud pressure is less than the ram pressure. It is assumed that the density of gas in the non-void medium (see Eq. 2) is,

$$\rho_{NV} \approx 2 \frac{\Omega_b}{\Omega_m} \rho_{crit}, \quad (4)$$

where $\rho_{crit} = 3H^2/8\pi G$, a function of redshift. This value is in recognition of the fact that this region is undergoing a mildly non-linear collapse, and therefore the average density should be mildly super-critical – *ie.*, $\sim 2 \rho_{crit}$.

In Fig. 3 I show the results of subjecting un-stripped model clouds (top line in each panel) to ram pressures of a gas of the above density, and outfall velocities 25, 50, 100, and 200 km s^{-1} .

2.2. Bow Shock Stripping

When the cloud outfall velocity is greater than the sound speed of the ambient medium, a bow shock will result. I assume the IGM has an average temperature $T_{NV} = 10^4$ K, consistent with an adiabatic sound speed of $c_s \sim 17$ km s^{-1} . This temperature is consistent with the simulation of Davé & Tripp (2001) for an over-density $\sim 4 \rho_{crit}$. In sustaining the first shock, the cloud has been stripped down to a volume within which the pressure is greater than the ram pressure of the shock. From this point, a quasi-stable situation results; a bow shock is set up which stands off some distance from the cloud proper. The ambient gas penetrates the shock, and is compressed and heated, according to the Rankine-Hugoniot jump conditions, producing a shear layer that meets with the cooler, denser medium of the cloud. There is a high-pressure zone at the head of the cloud due to the presence of the moving cloud immediately behind it, causing gas to be diverted around it. Gas is then accelerated down the flanks of the cloud by the pressure differential. The transverse motion over the cooler and denser cloud body may cause Kelvin-Helmholtz (K-H) instabilities which could strip away the cloud, layer by layer.

For plane shocks in the Mach range of $3 \leq \mathcal{M} \leq 6$ (~ 50 to 100 km s^{-1}), the velocity inside a plane shock has Mach numbers ranging from 0.49 to ~ 0.46 , respectively. Oblique shocks produce higher Mach values inside the shock. This fact, plus the pressure gradient along the length of the cloud inside the bow shock means that the velocity transverse to the cloud may substantially exceed Mach 0.5, perhaps by a factor of 1.5 or so. At the same time, the contrast between the average cloud density in the un-stripped part of the cloud and the gas between the cloud and the bow-shock varies from ~ 50 to 64 to 90, for $v_{cl} = 50, 75,$ and 100 km s^{-1} , respectively. According to the 1-D analysis of Vietri et al. (1997), the growth rate of K-H perturbations at $0.7 \leq \mathcal{M} < 1.0$ is essentially zero for adiabatic fluids when the density contrast between the cloud and the stripping medium is on order 100. These considerations suggest that stripping rates are low for the outfall velocities we are considering.

Anecdotal evidence also suggests that clouds may endure the stripping of the diffuse IGM gas for long periods without significant mass erosion. For instance, the very existence of the Local Group cloud compact high velocity cloud CHVC 125+41-207 at a distance $50 \lesssim d \lesssim 137$ kpc (Brüns et al., 2001), with its dense core and a long tail, strongly suggests it has survived billions of years of stripping. For, since CHVCs are found to have an average velocity ~ -100 km s^{-1} relative to the barycenter of the Local Group (Braun & Burton, 1999), this cloud would have to have existed for up to ~ 10 Gyr in order to have moved a Local Group diameter of ~ 1 Mpc. Since there is no conceivable way of creating this cloud within the Local Group in recent times, we must conclude that it has been traveling through the IGM at a similar velocity for a time on order 10 Gyr, retaining much of its mass. Thus this and other CHVCs may be ancient objects that have survived billions of years of bow shock stripping; they could be the dissipatively stripped and compacted ancestors of secondary infall, as explained in the scenario of Manning (1999).

While it is reasonable to postulate that smaller clouds might not endure this stripping as long as larger clouds, there is no way at present, short of detailed hydro/gravity simulations, to precisely determine the lifetimes of clouds under bow shock stripping. However, we may assume they all survive on order 10 Gyr, understanding that this may over-estimate the quantity of surviving clouds in non-void space at the present time. However, since clouds with low halo velocities are stripped much more efficiently by shocks, large clouds dominate the cross-section of absorbers at the velocities relevant in this problem, so that small clouds will have only a small effect on results in any case.

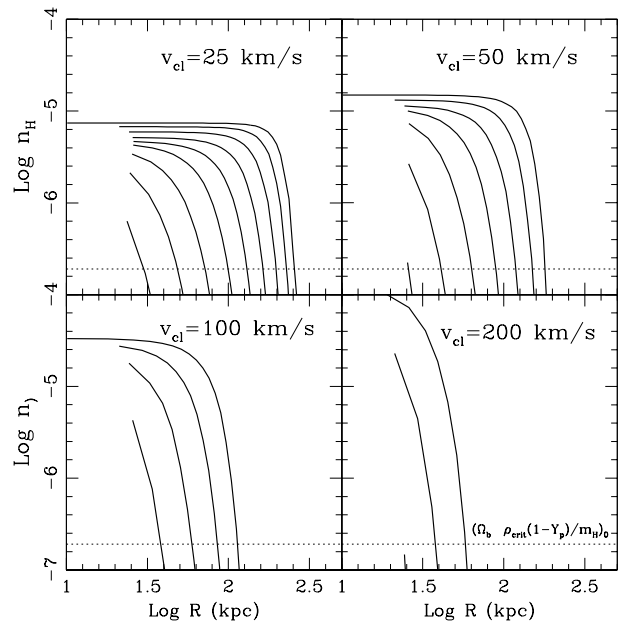


FIG. 4.— The density profiles resulting from the redistribution of baryons to an average density within the zone where the cloud pressure is greater than the ram pressure, then smoothed at the edge with same exponential used in Eq. 3. Shown are the distributions for the range of halo velocities noted in §2.3, in ascending order, left to right. These profiles provide the fiducial cloud model for the calculation of the non-void CDS.

2.3. Turbulent Mixing of the Surviving Cloud

In the globular cluster formation model of Manning (1999), the internal baryonic density of self-gravitating clouds that are stably responding to supersonic winds (*i.e.*, clouds are large enough to survive both stages of stripping) must increase with time. This is partly due to the deceleration of the cloud by ram pressure, but is also the result of a cycle of pressure-heating at the front-end of the cloud, and radiative cooling, as the denser cloud gas is pushed along toward the trailing end of the cloud by the shear wind. The K-H instabilities may gradually introduce an orderly, toroidal convection pattern in the cloud. This physical picture may be very similar for void clouds entering the non-void environment. The effect of both cloud deceleration (including a displacement of the baryonic cloud from its dark halo), and the fluid waves driven down the “fetch” of the cloud’s edge, is to disrupt the previous density profile within the truncation radius of the shock. In the simulations of MI94, the central condensation of the baryons within the bow shock is quickly lost. There are thus good grounds for assuming that the baryons within the shock (excepting the shear layer in between) become more evenly distributed; cloud containment switches from gravitational to pressure confinement when moving into non-void space.

For a large cloud, a velocity of 100 km s^{-1} will truncate the cloud at about 100 kpc (see Fig. 4). I use these values as fiducial in the calculation of the time-scale for the transformation from a void cloud to a non-void cloud. A useful conversion for the velocity is $100 \text{ km s}^{-1} \sim 100 \text{ kpc/Gyr}$. Thus, it would take $\sim 2 \text{ Gyr}$ for the cloud to pass completely into the dissipated gas of the filaments. During, and after the process of shock stripping, the baryonic cloud is being decelerated by the ram pressure. I calculate the time required for the baryonic cloud to be slowed enough for it to become displaced from the DM by one cloud radius. DM plays an important role in maintaining the central condensation of the cloud, and when it is gone, pressure gradients can quickly redistribute the gas. The deceleration caused by ram pressure is,

$$a = \frac{\rho_{NV}\pi(r_{cl}v_{cl})^2}{m_{cl}}. \quad (5)$$

I am interested in when the displacement is one cloud radius; $r_{cl} = 0.5 at^2$. Solving,

$$t = \left(\frac{r_{cl}}{v_{cl}}\right) \sqrt{\frac{8\rho_{cl}}{3\rho_{NV}}}. \quad (6)$$

Fiducial values for the density of dissipated gas in the IGM are, $\rho_{NV} = 2\Omega_b\rho_{crit}$, and $\rho_{cl} \approx 10\Omega_b\rho_{crit}$. Thus, since $r_{cl}/v_{cl} = 1 \text{ Gyr}$, $t \approx 3.6 \text{ Gyr}$. In §4, I show that the characteristic half-width of the transition zone is $\sim 0.5 \text{ Mpc}$ (for $0.1 \leq \mathcal{T} \leq 0.2$). For average cloud baryon densities $\bar{\rho}_{cl} \lesssim 20 \Omega_b\rho_{crit}$, the transition time-scale $t \lesssim 5 \text{ Gyr}$. The cloud thus moves less than the half-width of the transition zone by the time it is effectively flattened.

This general picture is confirmed by Fig. 2 of MI94; by the time of Figure 2 *d*, $\sim 1.7 \text{ Gyr}$ after the initial shock, a shear layer envelops a cloud with a flat density profile, bounded by sharp density gradients. The loss of the central condensation of this model cloud was accomplished in about one half the time estimated above.

It is thus expected that the clouds in “undisputed” non-void space (ie, $\log \mathcal{T} \gtrsim -0.7$; outside the transition zone) will approximate a flattened, or random mass distribution inside the shear layer of the cloud, so that the average density in random sightlines is independent of the cloud impact parameter. In the transition zone, one may find void clouds, clouds in various stages of the process of being transformed into non-void clouds.

To account for this effect in model clouds, I re-distribute the mass within the truncated cloud so that the density is uniform, but I apply the same exponential factor used in Eq. 3 to smooth the edges. In addition, the neutral fraction of hydrogen in the cloud must be “flattened” as well; I substitute the mass-weighted neutral fraction within the truncated cloud summed over each bin in the truncated cloud. Figure 4 shows the density profiles derived using this methodology for various outfall velocities v_{cl} . The halo velocities corresponding to the various lines in the figure are given by

$$v_c = 5.31 \times 10^{0.05n} \text{ km s}^{-1},$$

where $n = 16$ (*i.e.*, 33.5 km s^{-1}) for the far right-hand side line³, $n = 15$ for the next at 29.9 km s^{-1} , then 26.6, 23.7, 21.1 km s^{-1} , ..., and so on, for $n = 14, 13, 12$, etc.

3. MODELING THE NON-VOID CDS

The CDS is produced using a method very similar to that used to model the void clouds and the HVDF to produce the void CDS (§6, Paper II). The difference in treatment is that there is an extra variable – the cloud velocity v_{cl} that results in the stripping of clouds. Each model CDS is initially normalized using ϕ_V^* , the void LF normalization, and must be adjusted to approximate the observed CDS with a “concentration factor” f_{mult} , which is a function of cloud velocity.

The first step in modeling the non-void CDS is deciding which density profile of the shocked clouds works best. The upper panel of Fig. 5 shows normalized CDS for a shocked cloud ($v_{cl} = 100 \text{ km s}^{-1}$) in which the density profile is unadjusted, as in Fig. 3 (short-dashed line), one in which it is flattened, as in Fig. 4 (solid line), and an average of the two profiles (dot-dashed). This average is produced by simply averaging the number of H atoms in the respective Lagrangian bins of the unflattened and flattened clouds. Note that the range of legitimacy of this gas profile is expected to be confined to the transition zone since clouds are expected to be fully flattened by the time they emerge from it. These CDS are shown in relation to the observed non-void CDS ($\mathcal{T}_{lim} \geq 0.1$ (heavier jagged line)). For reference, the void CDS is represented by the long-dashed line. The quality of the fit to the CDS is consistently good over the range $75 \lesssim v_{cl} \lesssim 200 \text{ km s}^{-1}$.

These results suggest that the flattened ram-pressure stripped cloud profiles described above produce the best fit to the non-void CDS. Thus, results confirm expectations. I therefore adopt the flattened profiles as the preferred non-void cloud model, realizing it may not work well in the transition zone.

The next step is to constrain v_{cl} . The lower panel of Fig. 5 shows normalized model CDS multiplied by the

³in the modeling of Paper II, this is the largest halo to survive without inside-out collapse, and star formation

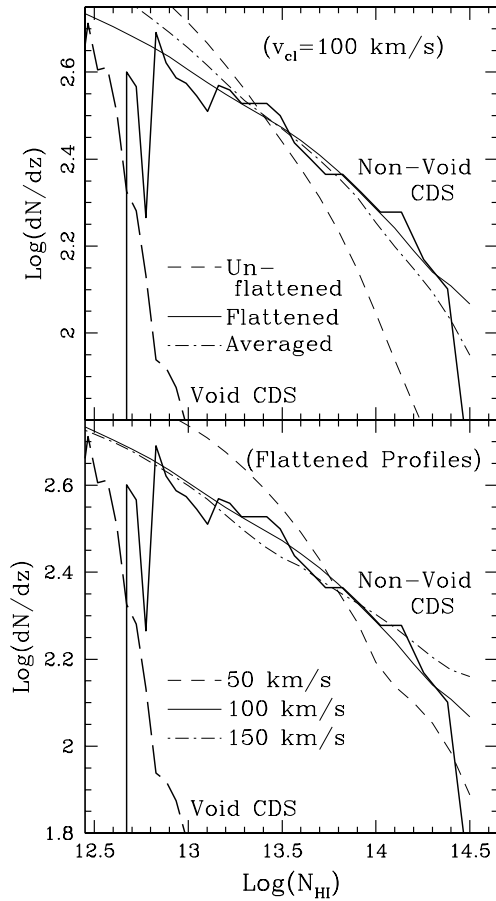


FIG. 5.— Normalized model column density spectra in relation to the observed non-void CDS (heavy solid line) and void CDS (heavy long-dashed line). The upper panel presents model CDS for unflattened halos (short-dash; profiles as in Fig. 3), flattened halos (thin solid line; profiles as in Fig. 4), and that resulting from a profile made by averaging the two (dot-dashed line). In this figure, the cloud velocity is $v_{cl} = 100 \text{ km s}^{-1}$. In the lower panel, model CDS are presented for various cloud velocities using flattened cloud profiles (as in Fig. 4). For $200 \gtrsim v_{cl} \gtrsim 75 \text{ km s}^{-1}$, these cloud profiles provide a good fit to the slope of the observed non-void CDS. The normalization factors f_{mult} are shown in Fig. 6.

adjustable factor f_{mult} based on cloud velocities of 50, 100, and 150 km s^{-1} , shown in comparison with the observed non-void CDS, as derived in Paper I. Note that the high quality of the fit to the observations shown when $v_{cl} = 100$ or 150 km s^{-1} , is absent for a velocity as low as 50 km s^{-1} .

Figure 6 shows the concentration factors f_{mult} required to adjust model CDS, with their void HVDF normalization, to match the observed non-void CDS for a range of cloud velocities. Such a concentration factor is the natural result of models of hierarchical clustering (e.g., Lacey & Cole, 1993).

It is possible to estimate the value of the concentration factor independently from the relative values of the normalizations of the HVDFs in void and non-void space. According to §7 of Paper II, the void CDS can be best explained with the HVDF of the “grown” halo cloud profiles, with slope parameter $\alpha \simeq -1.95$, and with normalization

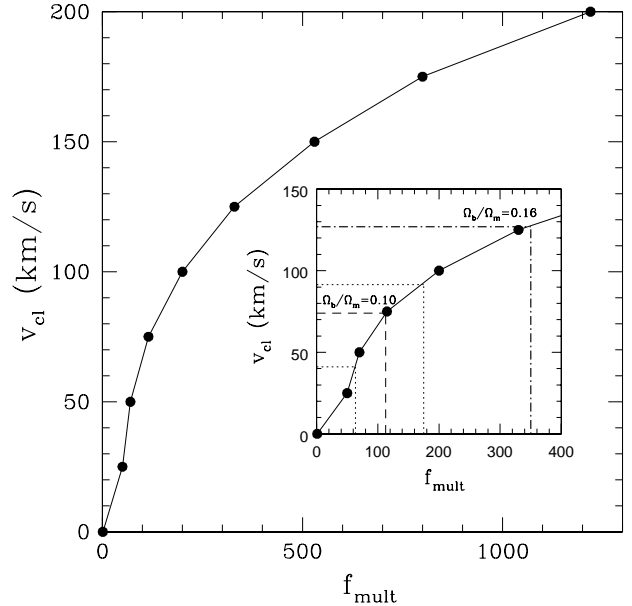


FIG. 6.— The relation between the cloud velocity v_{cl} , and the multiplicative factor f_{mult} necessary to fit the model CDS (made by simulating the stripping process) to that of the observed. The significance of the lines are explained in the text.

$\phi_V^* \simeq 0.06 \phi^*$ (§6, Paper II), where ϕ^* is the normalization of the mean luminosity function (LF). With the B -band LF, I use $\phi^* \simeq 0.022 \text{ h}^3 \text{ Mpc}^{-3} = 0.0093 \text{ h}_{75}^3 \text{ Mpc}^{-3}$ (Eq. 36 of Paper II). Knowing the filling factors, we can write the equation,

$$\phi_V^* f_V + \phi_{NV}^* f_{NV} = \phi^*, \quad (7)$$

where ϕ_{NV}^* is the normalization of the LF in the non-void space (again functionally identical to that of the region containing shocked gas), with filling fraction f_{NV} , and f_V is given by Eq. 1 (i.e., $f_{NV} = 1 - f_V$). Thus,

$$\phi_{NV}^* = \phi^* \frac{1 - f_V (\phi_V^*/\phi^*)}{f_{NV}} = 6.77_{-2.95}^{+3.73} \phi^*, \quad (8)$$

where the errors are propagated from the range in f_V in Eq. 1. Using the void normalization ϕ_V^* for the grown halos, the expected concentration factor required to arrive at the normalization of the non-void population (Eq. 8) would be

$$f_{mult} = \frac{\phi_{NV}^*}{\phi_V^*} \approx 113_{-49}^{+62}, \quad (9)$$

though this is subject to a few caveats (see below).

At this point it is convenient to consider how things would appear if I had used $\Omega_b/\Omega_m = 0.16$, consistent with the WMAP data (Spergel & colleagues, 2003), instead of 0.10 (§1). I re-ran the simulations discussed in Paper II using this new value, and derived the CDS, which is consistent with the observed void CDS. The fit was managed using the same faint-end slope parameter $\alpha = -1.95$, but the normalization was lower; $\phi_V^* \simeq 0.02 \phi^*$, $\sim 1/3$ of the value derived with the lower baryon density. These model clouds were analytically shock-stripped as described above, resulting in very similar values of f_{mult} for a given

v_{cl} ; apparently the larger cloud neutral fraction, and consequently larger cross-section at a given column density, make up for their lower indicative space density in voids when Ω_b is larger. However, because ϕ_V^* is now lower, Eqs. 8 and 9 have different values. The non-void normalization is slightly higher ($\phi_{NV}^* = 7.02_{-3.08}^{+3.88} \phi^*$) and the predicted concentration parameter is about 3 times higher ($f_{mult} \simeq 351_{-154}^{+194}$).

Due to the transferral of matter from void to non-void space, the distributions of halo velocities of void and non-void clouds are causally linked. If the slope of the HVDF does not change going from the unshocked to the shocked environments, and if void clouds are indeed the precursors of non-void clouds, then the multiplicative factor needed to adjust the CDS of stripped clouds to the observed non-void CDS is given by Eq. 9.

However, Eq. 9 should not be accepted uncritically. Klypin (2002) found that sub-halos have HVDFs consistent with a slope parameter $\alpha \simeq -1.72$, while isolated halos have $\alpha \simeq -1.95$ (see §6.2 of Paper II). This is suggestive of a flattening of the spectral slope in higher-density areas. If the observed non-void clouds have average halo circular velocities of $v_c \simeq 30 \text{ km s}^{-1}$, then for $\alpha = -1.72$, there would be 2.7 times fewer 30 km s^{-1} clouds in non-void space than if $\alpha = -1.95$. This, in turn, would require a reduction of f_{mult} by a factor ~ 2.7 . That is, Eq. 9 should, by rights, have been $f_{mult} = \phi_{NV}(v_c \sim 30)/\phi_V(v_c \sim 30)$, for the greater effect of stripping on small clouds results in the largest clouds providing the bulk of the cross-section of stripped clouds. However, we have no direct information on their number density in the IGM, as we do of \mathcal{L}^* galaxies. Though the higher densities of clouds in non-void space gives greater opportunity for hierarchical agglomeration and a consequent flattening of the spectral slope, these clouds are by no means generally sub-halos, for the overwhelming majority of non-void clouds in this survey are far outside the virial radius of any galaxy (see §4).

On the other hand, it is more plausible that \mathcal{L}^* galaxies, lying in dense zones of the filamentary structures, could have enhanced numbers (relative to the initial, but concentrated halo spectrum) due to hierarchical agglomeration of smaller halos – especially of sub-perturbations accreted during the primary collapse phase at $z \gtrsim 3$. I consider it plausible, therefore, that the f_{mult} applicable to clouds may be up to ~ 3 times smaller than quoted in Eq. 9.

Fig. 6 shows the trend of f_{mult} with v_{cl} neglecting this possible factor. Over the range of velocities of relevance to this study, the concentration factors for the larger baryon density ($\Omega_b/\Omega_m \sim 0.16$) are entirely consistent with those of the smaller baryon density. The inset shows a set of three vertical lines corresponding to the values of f_{mult} in Eq. 9, and imply cloud velocities in the range $42 \lesssim v_{cl} \lesssim 91 \text{ km s}^{-1}$. The dot-dashed line represents the central value of f_{mult} when $\Omega_b/\Omega_m = 0.16$, implying a central value $v_{cl} \approx 130 \text{ km s}^{-1}$, and a range $100 \lesssim v_{cl} \lesssim 150 \text{ km s}^{-1}$.

As noted above, the considerations of hierarchical merging in dense zones suggest that f_{mult} , as calculated by Eq. 9, may be less than indicated by Eq. 7 (*i.e.*, 113 and 350 km s^{-1} for $\Omega_b/\Omega_m = 0.10$ and 0.16, respectively), perhaps by a factor on order 3, although the relative isolation of most non-void clouds suggest it is a small fraction of

this. According to Fig. 6, this would imply a significantly smaller velocity. For $\Omega_b/\Omega_m = 0.10$, this would imply a velocity $v_{cl} \ll 50 \text{ km s}^{-1}$. Recall, however, that the quality of the fit of the model non-void CDS to the observed declines when $v_{cl} \lesssim 75 \text{ km s}^{-1}$. For the larger Ω_b , cloud velocity could be expected to drop from $\sim 130 \text{ km s}^{-1}$ to $\gtrsim 80 \text{ km s}^{-1}$, and still give a good fit to the observed CDS slope.

The one thing that may argue against this whole logical construct is, of course, that non-void clouds can be understood in terms of a FGPA. I visit this issue in the next section.

4. DISCUSSION AND SUMMARY

Further discussion in three broad areas is needed to tie this investigation together; the FGPA, the transition zone, and the line-density of absorbers as a function of \mathcal{T} in non-void space.

4.1. FGPA

It was shown in §1 that the predictions of the FGPA for the IGM do not appear to agree with observations. The presence of many clouds in void space (Paper I) stands in contrast with their relative absence under the FGPA. Their absorbers are produced in the slowly varying dissipated gas of the filamentary structure surrounding galaxy concentrations. However, the distribution of clouds proponents predict is inconsistent with the observed distribution of clouds in the same non-void locale (see Fig. 2). These indicate a significant problem with the standard model of low- z Ly α clouds, and hence, by extension, perhaps also with that of the high- z Ly α forest.

Although the present work has shown that non-void clouds may be explained by the effects of shocks on previously unshocked void clouds, this does not mean that none of the absorbers have their origin in an FGPA. The above analysis suggests that if they do exist, the FGPA absorber Doppler parameters should be larger than those of sub-galactic halos, which are essentially self-gravitating and whose integration path lengths are smaller. Similarly, it appears likely that the prediction of very low column density clouds in the IGM is due to an incorrect assessment of the Doppler parameters. For among the initial assumptions of the FGPA is that of neglecting turbulent effects within the line (which is already broadened by relative velocities of order 10 to 40 km s^{-1}), as explained in Bi (1993). Required integration path lengths are on order 1 Mpc at $z \sim 0$ (Paper II). It seems improbable that in a turbulent medium there would not be a broadening of the spectral absorption lines over distance such as this.

What sources for turbulence might there be? If the ‘‘Birkhoff’’ effect is propelling centrally condensed clouds into the IGM, this represents a major source of kinetic energy to drive the turbulence. On the high \mathcal{T} -side of the non-void universe, energy injection comes with superwinds from post-starburst galaxies and the like. If turbulent motions of $\sim 100 \text{ km s}^{-1}$ (v_{cl}) exists over scales of 200 kpc ($2r_{cl}$), then over megaparsec scales, a significant turbulent dispersion of absorption lines on order $\gtrsim 100 \text{ km s}^{-1}$ would be plausible. Their Doppler parameters are in fact large enough to make the lines appear as a continuum depression. Since FGPA integration path lengths are weakly

correlated with column density, FGPA Doppler parameters should be rather uniformly $\gtrsim 100 \text{ km s}^{-1}$. By contrast, the Doppler parameter histogram of non-void clouds finds $b \simeq 60 \text{ km s}^{-1}$ with a dispersion of 15 km s^{-1} or so (Fig. 7 of Paper I; Fig. 15b of Paper II). These histograms show no sign that there is a higher- b component of absorbers. In fact, the 60 km s^{-1} broadening seems appropriate for a centrally condensed cloud undergoing a dissipative interaction with the IGM. Thus, there is no sign of FGPA clouds at $b \lesssim 100 \text{ km s}^{-1}$, the upper-limit for the Penton et al. (2000) data.

4.2. The Transition Zone

Much of the modeling of non-void clouds depends on the physical picture of a sudden transition from a cool diffuse void to a warm, relatively dense, and turbulent IGM. Let us consider this picture in some detail, motivated by the following question: why should non-void space have a relatively abrupt end, so that clouds are quickly shock-stripped? The fundamental fact about the edge of voids is that, on the one hand, diffuse, adiabatically cooled matter is balanced by a denser and warmer gas on the other. Obviously, the pressure in the latter p_{NV} is much greater than that in the former p_V . The pressure difference will cause an expansion of the IGM into the diffuse void gas. Alternatively, the fact that the local expansion parameter in voids is greater than the mean, suggests that we may consider that the cool, diffuse gas is flowing into the denser gas at a velocity sufficient to cause stationary shock front. The equation for pressure balance is then,

$$\rho_V v_{out}^2 = p_{NV} - p_V, \quad (10)$$

where $v_{out} = (H_V - H_0)R_V$. Solving for v_{out} in Eq. 10,

$$v_{out} = \sqrt{\frac{k}{\mu m_H} \left(\frac{\rho_{NV} T_{NV}}{\rho_V} - T_V \right)}. \quad (11)$$

The ambient temperature of non-void space is assumed to be 10^4 K (see §2.2), while the adiabatically cooled void space is $\sim 3000 \text{ K}$ (Paper II, §4.3 and Fig. 5). We further assume the average gas densities are,

$$\begin{aligned} \bar{\rho}_V &= 0.1 \Omega_b \rho_{crit}, \\ \bar{\rho}_{NV} &= 2.0 \frac{\Omega_b}{\Omega_m} \rho_{crit}, \end{aligned}$$

where the former suggests the background (unclustered) density of baryons is a tenth of the mean, while the latter is Eq. 4. Thus, $\rho_{NV}/\rho_V \sim 67$ when $\Omega_m = 0.3$. These values imply that

$$v_{out} \simeq 95 \text{ km s}^{-1}.$$

That is, an outfall velocity of $v_{out} \sim 95 \text{ km s}^{-1}$ will maintain a pressure discontinuity consistent with what was presumed here. This accounts for the strong density gradient at the boundary between void and non-void space, and the apparent rapidity of the onset of shock stripping on clouds; it helps confirm the self-consistency of the physical picture.

4.3. The Non-Void Cloud Spatial Distribution

I now consider what might be learned from the trend of the cumulative line density of Ly α absorbers as a function of \mathcal{T}_{lim} . The trend in the log of the intercept C in Fig. 1B for the non-void EWDFs (solid line, right-hand side of upper sub-panel of panel b) appears to be well-fit by a line. I find that the trend is consistent with a cumulative line density at $\mathcal{W} = 63 \text{ m\AA}$ of $d\mathcal{N}(\geq \mathcal{T}_{lim})/dz = 783 \mathcal{T}_{lim}^{0.394}$. The figure shows that this relation is accurate over the range $0.1 \lesssim \mathcal{T} \lesssim 4$. The slope may be taken to give information about the radial distribution of clouds about isolated galaxies, for the steep dependence of tidal field strength with distance from galaxies essentially ensures that high tidal field regions are close to a strong concentration of mass. Consider an isolated, centrally condensed body. It follows that the tide varies as $\sim R^{-3}$ (Eq. 17b of Paper I)⁴, so that the cumulative line density is $d\mathcal{N}(\leq R_{lim})/dz \propto R_{lim}^{-1.18}$, where R_{lim} is the distance at which $\mathcal{T} = \mathcal{T}_{lim}$. This implies a differential line density $d^2\mathcal{N}(R)/dz dR \propto R^{-2.18}$. If the radii of clouds within the IGM do not vary systematically with tidal field, then the number density of clouds is proportional to the differential line density. This exponent, -2.18 , is quite close to that derived for the distribution of satellite galaxies around isolated parent galaxies found by McKay et al. (2002); $n \propto R^{-2.1}$ – a relation valid in the range $133 \lesssim R \lesssim 670 \text{ h}_{75}^{-1} \text{ kpc}$. For a case in which tides are caused by an \mathcal{L}^* galaxy ($v_c \simeq 161 \text{ km s}^{-1}$; Tully & Pierce 2000), with Eqs. 14 and 16 of Paper I, it can be shown that scalar tidal fields in the range $0.1 \lesssim \mathcal{T} \lesssim 4$ (inverse Hubble times squared) would be produced at a distance $730 \lesssim R \lesssim 2500 \text{ h}_{75}^{-1} \text{ kpc}$. For reference, the high \mathcal{T} -side of the transition zone ($\mathcal{T} \simeq 0.2$ would occur $\sim 2 \text{ Mpc}$ from an \mathcal{L}^* galaxy, making the half-width of the transition zone $\sim 0.5 \text{ Mpc}$).

The lower limit of the tidal field range is enticingly close to the upper limit of the McKay *et al.* range. If these clouds trace mass, then this apparently quite extended, though sparse, “halo” of non-void clouds about galaxies may represent an extension of the mass distribution entailed by the flat velocity dispersions around giant field galaxies that extend out to $R_p \simeq 670 \text{ h}_{75}^{-1} \text{ kpc}$ (McKay et al., 2002). If this is so, then there is a chance to calibrate how cloud number densities trace matter density. This may eventually lead to an estimate of the void matter density.

This analysis strongly suggests that the observed CHVC population, thought to be dark matter-held (Blitz et al., 1999; Sternberg et al., 2002), and with an average Local Group barycentric motion of -100 km s^{-1} (Braun & Burton, 1999), are representatives of sub-galactic halos that have accreted to the IGM long ago. They are, I would suggest, the closest examples of the discrete clouds which constitute the non-void column density spectrum.

5. SUMMARY

A self-consistent picture has been built that uses shock-stripping in the IGM (non-void space) to transform void

⁴As noted in §5.1 of Paper I, galaxies are taken to extend to the truncation radius R_t , assumed to be $500 \text{ h}_{75}^{-1} \text{ kpc}$ for an \mathcal{L}^* galaxy. In calculating tidal fields, the galaxy mass is summed to R_t , and the tide is calculated as though it were a point mass. Thus the above method is consistent even within R_t .

clouds into non-void clouds. A connection between the relative LF normalizations of the HVDFs in void and non-void space was used to calculate a “concentration factor” that adjusts the CDS of transformed model void clouds for the convergent concentration of clouds into the more compact non-void space of the IGM. Whether the concentration factor can successfully explain the observed non-void CDS depends on the cloud velocity and the attendant ram-pressure stripping. I have shown that non-void clouds are consistent with shock stripped void clouds when this correction factor is employed. When cloud velocities $v_{cl} \gtrsim 75$ km s^{-1} , the shape of the model CDS derived here is in excellent agreement with the observations when the baryons in shocked clouds lose their central condensation and become evenly distributed inside the shear layer. Mergers in dense regions of non-void space may increase the number density of \mathcal{L}^* -galaxies, a change which is accompanied by a lowering of the “faint-end” slope parameter α . This suggests fewer clouds in non-void space (by up to $\sim 1/3$), lowering f_{mult} , and suggesting lower outfall velocities. For the lower baryon density initially assumed for this and previous papers, the implied velocity could be less than 50 km s^{-1} , but does not produce a CDS that fits well with observations. However, for the larger baryon density consistent with the WMAP results, $v_{cl} \approx 100$ km s^{-1} appears consistent from the standpoint of the quality of the fit to the observed non-void CDS, and the implied concentration factor f_{mult} .

Indications from the systematic velocity of CHVCs, and from the requirements of maintaining a strong pressure gradient between void space and the non-void environment, appears to require a void “outfall” velocity on order $v_{out} \approx 100$ km s^{-1} .

6. ACKNOWLEDGMENTS

I wish thank Christopher F. McKee for many helpful comments and suggestions. I thank Hy Spinrad for financial support and for his wisdom during his stint as my research advisor. I received financial support of NSF grant #AST-0097163 and the UC Berkeley Department of Astronomy.

REFERENCES

- Bi, H. 1993, ApJ, 405, 479
 Birkhoff, G. D. 1923, *Relativity and Modern Physics* (Cambridge, Mass: Harvard University Press)
 Blitz, L., Spergel, D. N., Teuben, P. J., Hartmann, D., & Burton, W. B. 1999, ApJ, 514, 818
 Brüns, C., Kerp, J., & Pagels, A. 2001, A&A, 370, L26
 Braun, R. & Burton, W. B. 1999, A&A, 341, 437
 Cen, R. & Ostriker, J. P. 1999, ApJ, 514, 1
 Croft, R. A. C., Weinberg, D. H., Katz, N., & Hernquist, L. 1998, ApJ, 495, 44
 Davé, R. & Tripp, T. M. 2001, ApJ, 553, 528
 Davé, R., Hernquist, L., Katz, N., & Weinberg, D. H. 1999, ApJ, 511, 521
 Klypin, A. 2002, Modern Cosmology, ed. S. Bonometto, V. Gorini, & U. M. (eds) (Bristol and Philadelphia)
 Klypin, A., Kravtsov, A. V., Valenzuela, O., & Prada, F. 1999, ApJ, 522, 82
 Lacey, C. & Cole, S. 1993, MNRAS, 262, 627
 Manning, C. V. 1999, ApJ, 518, 226
 —. 2002, ApJ, 574, 599
 —. 2003, ApJ, 591, 79
 McKay, T. A., Sheldon, E. S., Johnston, D., Grebel, E. K., Prada, F., Rix, H., Bahcall, N. A., Brinkmann, J., Csabai, I., Fukugita, M., Lamb, D. Q., & York, D. G. 2002, ApJ, 571, L85
 Miralda-Escude, J., Cen, R., Ostriker, J. P., & Rauch, M. 1996, ApJ, 471, 582
 Murakami, I. & Ikeuchi, S. 1993, ApJ, 409, 42
 —. 1994, ApJ, 420, 68
 Navarro, J. F., Frenk, C. S., & White, S. D. M. 1996, ApJ, 462, 563
 Navarro, J. F., Frenk, C. S., & White, S. D. M. 1997, ApJ, 490, 493
 Penton, S. V., Stocke, J. T., & Shull, J. M. 2000, ApJS, 130, 121
 Piran, T. 1997, General Relativity and Gravitation, 29, 1363
 Prada, F. & colleagues. 2003, ApJ submitted, astro-ph/0301360
 Rees, M. J. 1986, MNRAS, 218, 25P
 Riediger, R., Petitjean, P., & Mucket, J. P. 1998, A&A, 329, 30
 Seldner, M. & Peebles, P. J. E. 1977, ApJ, 215, 703
 Spergel, D. N. & colleagues. 2003, ApJ submitted, astro-ph/0302209
 Sternberg, A., McKee, C. F., & Wolfire, M. G. 2002, ApJS, 143, 419
 Thoul, A. A. & Weinberg, D. H. 1995, ApJ, 442, 480
 Tully, R. B. & Pierce, M. J. 2000, ApJ, 533, 744
 Vietri, M., Ferrara, A., & Miniati, F. 1997, ApJ, 483, 262
 Weinberg, D. H., Hernquist, L., Katz, N., Croft, R., & Miralda-Escudé, J. 1997, in 13th IAP Astrophysics Colloquium: Structure and Evolution of the Intergalactic Medium from QSO Absorption Line System, 133
 Zabludoff, A. I. & Mulchaey, J. S. 2000, ApJ, 539, 136
 Zaritsky, D., Smith, R., Frenk, C., & White, S. D. M. 1997, ApJ, 478, 39
 Zaritsky, D. & White, S. D. M. 1994, ApJ, 435, 599